Assessment of CHF Characteristics at Subcooled Conditions for the CANDU CANFLEX Bundle

E. N. Onder and L.K.H. Leung

Atomic Energy of Canada Limited (AECL), Chalk River Laboratories, Chalk River, Ontario Canada K0J 1J0.

ondern@aecl.ca; leungl@aecl.ca

ondernagaeer.ea, reangragaeer.ea

ABSTRACT

An analysis has been performed to assess the Critical Heat Flux (CHF) characteristics for the CANFLEX¹ bundle at subcooled conditions. CHF characteristics for CANDU² bundles have been established from experiments using full-scale bundle simulators. These experiments covered flow conditions of interest to normal operation and postulated loss-of-flow and small break loss-of-coolant accidents. Experimental CHF values obtained from these experiments were applied to develop correlations for analyses of regional overpower protection and safety trips. These correlations are applicable to the saturated region in the reference uncrept channel and the slightly subcooled region in postulated high-creep channels. Expanding the CHF data to subcooled conditions facilitates the evaluation of the margin to dryout at upstream bundle locations, even though dryout occurrences are not anticipated there. In view of the lack of experimental data, the ASSERT-PV subchannel code has been applied to establish CHF values at low qualities and high subcoolings (thermodynamic qualities corresponding to -25%). These CHF values have been applied to extend the CHF correlation to the highly subcooled conditions.

KEYWORDS

CHF, CANFLEX Bundle, Subchannel Code, ASSERT-PV

1. INTRODUCTION

Accurate predictions of critical heat flux (CHF) are essential in regional overpower trip and safety analyzes of the CANDU reactors. CHF values for CANDU bundles are predicted using correlations derived from full-scale bundle data obtained with high-pressure steam-water flow. Supplemental CHF data were also obtained with refrigerant flows for comparisons of the CHF characteristics for various fuel bundle designs [1].

The CHF correlation for the CANFLEX bundle was derived with full-scale water experimental data covering CANDU 6 conditions in reference (uncrept) channel, 3.3% (mid-life) and 5.1% (maximum, or end-of-life) crept channels. These data covered the pressure range from 6 to 11 MPa, a mass-flux range from 2.7 to 6.7 Mg m⁻² s⁻¹, and a quality range from -0.06 to 0.32. The data ranges bound conditions encountered in postulated loss-of-regulation, loss-of-flow, and small break loss-of-coolant accidents, and hence are directly relevant and applicable for safety analyzes.

Currently, analytical tools are applied in the analysis of regional overpower and safety trips. The fuel string is subdivided into nodes, where local flow conditions are evaluated and applied in establishment of CHF. While dryout occurrences are not anticipated at highly subcooled conditions in upstream

¹ CANFLEX* (CANdu FLEXible) is a registered trademark of Atomic Energy of Canada Limited (AECL) and Korea Atomic Energy Research Institute (KAERI).

² CANDU[®] (CANada Deuterium Uranium) is a registered trademark of AECL.

locations, the evaluation process requires the CHF prediction. For completeness, the CHF correlation is extended to provide realistic predictions at highly subcooled conditions.

The objective of this study is to extend the applicability of the CANFLEX CHF correlation, which was derived using data obtained mostly in the saturated boiling region, to highly subcooled conditions. With the lack of experimental data in the subcooled region, the ASSERT-PV subchannel code was used to obtain CHF values.

2. METHODOLOGY

AECL³ has developed the ASSERT-PV code for examining subchannel flow and enthalpy behaviours in CANDU fuel bundles [2] and [3]. The code is generally used as a design assist tool for new designs of CANDU fuel bundles to predict pressure drop and dryout power in CANDU fuel channels [4] and provides support for safety and licensing codes. It has been validated against experimental data for the 37-element and CANFLEX bundles. The input file, previously applied in the validation exercise, was used in this work.

The CHF correlation for the CANFLEX bundle was developed with experimental data obtained with a full-scale bundle simulator at Stern Laboratories (SL) [5]. ASSERT-PV was applied in predicting the dryout power data to demonstrate its accuracy for the CANFLEX Mk-V bundle. It was then applied to predict dryout powers in the subcooled boiling region (through adjusting the inlet fluid temperatures). The boiling length average (BLA) CHF values and local flow conditions at dryout locations were compiled. These predicted values were compared against the experimental CHF values to establish the systematic bias over the range of SL experimental conditions. The prediction bias was eliminated and the corrected CHF values were applied in development of a correlation for the highly subcooled region. The two CHF correlations for the saturated and highly subcooled regions are combined into a single correlation for implementation into the safety analysis code.

3. STERN LABORATORY CANFLEX EXPERIMENTS

Dryout power experiments were performed with the bundle simulator installed inside the horizontal test station [5].

Figure 1 illustrates the horizontal test station and pressure-tap locations. Three different flow tubes were used in the test to house the bundle simulator; one had a uniform inside diameter of 103.86 mm, the other two had axially varying inside diameters, with maximum diameters of 107.29 mm and 109.16 mm (see Figure 3).

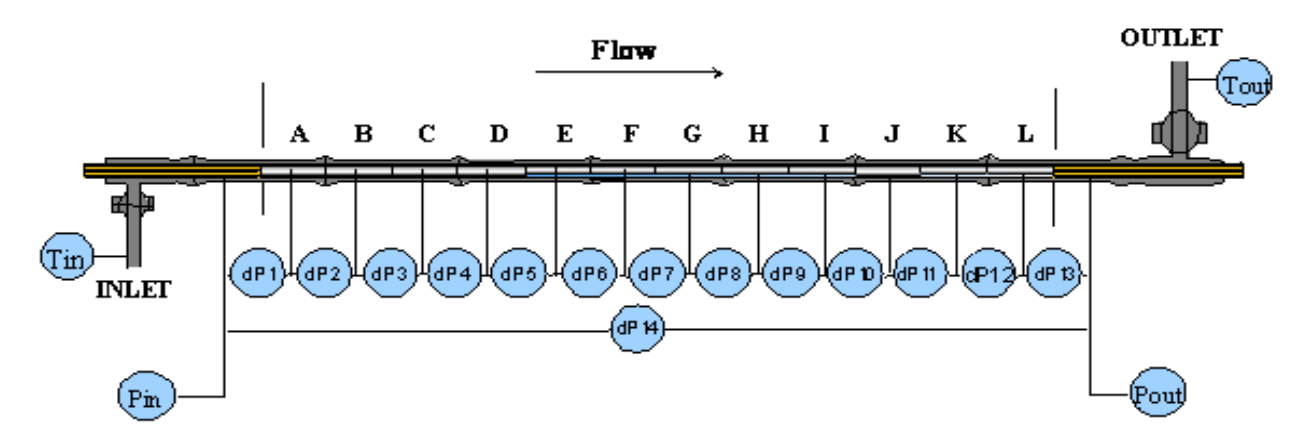


Figure 1: Stern Laboratories Horizontal Test Section with Pressure Taps

³ Atomic Energy of Canada Limited

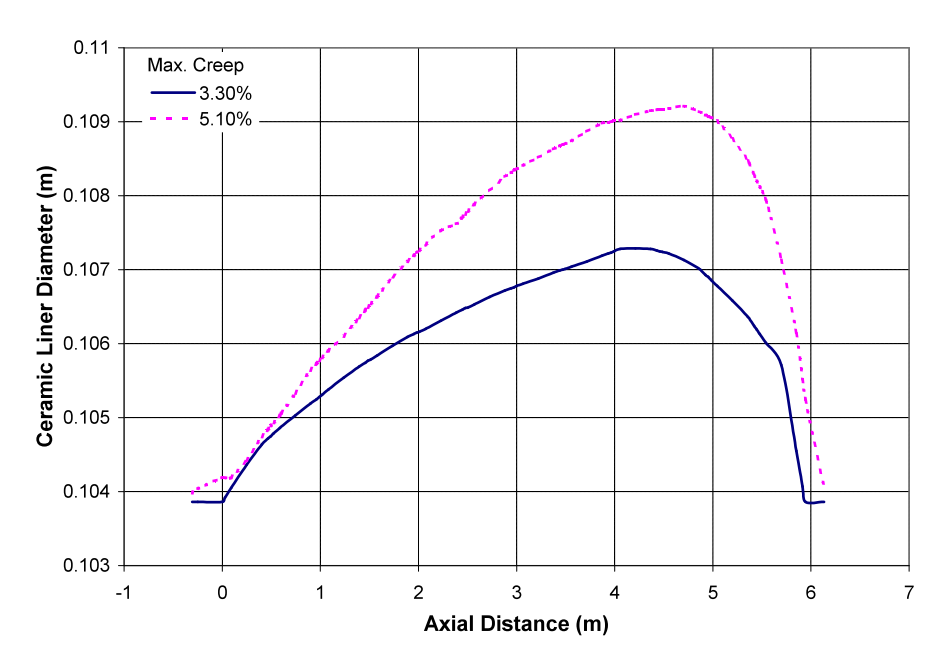


Figure 3: Flow Tubes of Axially Varying Inside Diameters

The 6 m long (nominal) electrically heated bundle simulator was constructed to simulate as closely as possible the external shape and dimensions of a string of 12-aligned CANFLEX bundles with end-plates, bearing pads, CHF enhancement buttons and spacers. Figure 4 shows the cross-sectional geometry of bundle simulator with appendages. In the experiments, two different bearing pad heights (1.7 mm and 1.8 mm) were used to quantify the effect of bearing pad height on the dryout power. The simulator was kept eccentric inside the flow tube using tunnel spacers and stainless-steel springs simulating the gravity effect on the bundle in a horizontal channel.

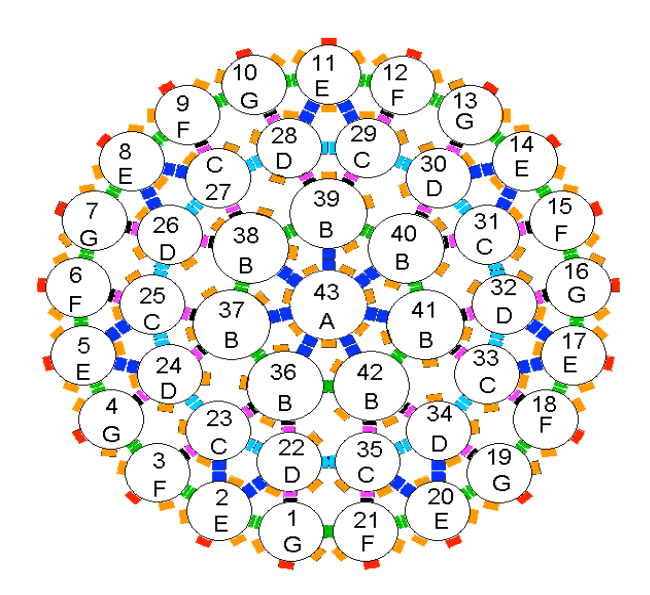


Figure 4: Cross-Sectional Geometry of Bundle Simulator with Appendages

The test section was heated with a DC power supply having an electrical capacity of 13.5 MW at a maximum of 240 volts. The tube wall thickness was varied over the length of the bundle string and among the ring elements to provide the non-uniform axial and radial heat-flux distributions (AFD and

RFD). The RFD corresponds to the profile exhibited in fresh natural uranium (NU) fuel. Figure 5 shows the tested AFD

Stern Laboratories Non-Uniform Axial-Flux Profile

Figure 5: Axial Flux Distribution

3.1 Instrumentation and Data Acquisition System

At the inlet and outlet sections, the fluid temperatures were measured using Resistance Temperature Detectors (RTD), and the absolute pressures using capacitance type pressure transmitters. Differential pressures were measured over a 0.4953 m length with capacitance type transmitters. Figure 1 shows the pressure-tap locations along the bundle string. The coolant flow was measured using two orifice meters in series.

Bundle string elements were equipped with 258 thermocouples mounted in movable ceramic carriers. Most of the thermocouples were located at the downstream of the bundle string, as the dryout was expected to occur at the downstream end of the simulator. These thermocouples were moved axially during the test to obtain surface temperatures at various locations of each element.

3.2 CHF Tests

At a given set of flow conditions (i.e., outlet pressure, inlet temperature and flow rate), the power was increased in steps until a sharp rise in sheath temperature detected at any thermocouples in the simulator (dryout was reached). Once the CHF was detected, the bundle power was increased by 50-100 kW and confirmation map tests were performed at the axial planes where it was considered that dryout might occur to ensure the dryout was not missed. CHF experiments were carried out at pressures varying between 6 and 11 MPa, mass flow rates between 10 and 25 kg s⁻¹, and inlet fluid temperatures between 200 and 290°C.

4. ASSERT-PV CODE AND SIMULATIONS

ASSERT-PV has been developed at AECL to meet the specific requirements for subchannel thermalhydraulic analysis of two-phase flows in horizontally oriented CANDU fuel bundles. It provides detailed flow and phase distributions in subchannels of a fuel bundle to evaluate CHF, post-dryout heat transfer, and fuel-sheath temperature.

The current release version of ASSERT-PV is ASSERT-PV V3R1 [3], which was used to predict dryout power in the present analysis. ASSERT-PV [3] is based on ASSERT-IV [2], which in turn

originated from the COBRA-IV computer program. The two-phase flow model used in ASSERT-PV is based on an advanced drift-flux model: a five-equation model that can consider thermal non-equilibrium and the relative velocity of the liquid and vapour phases. Thermal non-equilibrium is dealt with by two-fluid energy equations for the liquid and vapour. Relative velocity is obtained from semi-empirical correlations. While retaining the major features in ASSERT-IV, ASSERT-PV employs the more comprehensive and robust numerical solution based on the Pressure-Velocity numerical method to enhance the modelling capability under relatively low flows, among other ASSERT-PV improvements. The most up-to-date subchannel flow and enthalpy distribution models in ASSERT-PV are described in [7] including the single- and two-phase inter-subchannel turbulent mixing, void drift and diffusion, buoyancy drift, and the effect of bundle appendages.

Figure 6 illustrates the subchannel set-up and identification numbers in the ASSERT-PV simulation of the CANFLEX bundle. Dryout is considered to occur when the local heat flux at any one of these subchannels reaches the predicted CHF for that subchannel. ASSERT-PV predicts the CHF using the LW-T-1996 CHF table [8], and its associated correction factors for diameter, gap size and flow orientation effects, based on the local subchannel-flow conditions.

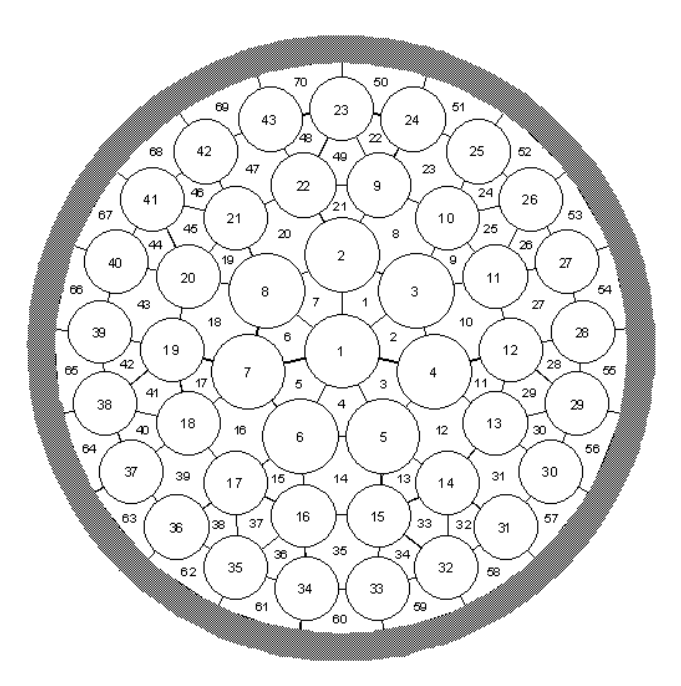


Figure 6: Subchannel Set-Up and Identification for the CANFLEX Bundle

4.1 Assessment of ASSERT-PV against SL CANFLEX Bundle Data

The ASSERT-PV code was assessed against the SL data obtained using CANFLEX bundle with 1.8 mm bearing pad height for the prediction accuracy of the dryout power. SL experiments [5] performed at 9 and 11 MPa outlet pressure in the channels with the maximum creep ratios of 0% (uncrept) and 5.1% were used for simulations.

The SL experiments showed that the initial dryout occurred in the outer ring at the bottom (elements 2, 3 and 21 in Figure 4) and at the horizontal symmetry (element 6 in Figure 4) of the tube, mostly in bundles 10 and 11, regardless of the channel creep. ASSERT-PV predicted the initial dryout in the inner-ring (element 6 in subchannel 15 in Figure 6) in bundles 11 and 12 for the 5.1% crept channel simulations, and in the inner-ring (element 6 in subchannel 15 in Figure 6) and in the outer-ring

(element 32, 34 and 35 in subchannels 34, 36 and 38 in Figure 6) in bundles 10, 11 and 12 for the uncrept channel runs. The outer-ring dryout predictions for the uncrept channel simulations were obtained at high flows $(21 - 22 \text{ kg s}^{-1})$.

Figure 7 compares dryout powers between the measured and predicted values in the uncrept and 5.1% crept channels. ASSERT-PV tends to overpredict dryout powers in both uncrept and 5.1% crept channels. Better predictions are obtained in the crept channel than in the uncrept channel. The overall average error is 4.9% and the associated uncertainty is 5.5% for all data, 2.4% and 4.3% for the 5.1% crept channel, and 6.3% and 5.6% for the uncrept channel, respectively. The average error is defined as:

Average Error =
$$\overline{\text{Error}} = \frac{1}{n} \sum_{i=1}^{n} (\text{Error})_{i}$$
 (1)

where the prediction error is defined as:

$$Error = \frac{Predicted Value}{Experimental Value} - 1$$
 (2)

The standard deviation is defined as:

Standard Deviation =
$$\sqrt{\frac{1}{n-1}} \sum_{i=1}^{n} (Error - \overline{Error})^2$$
 (3)

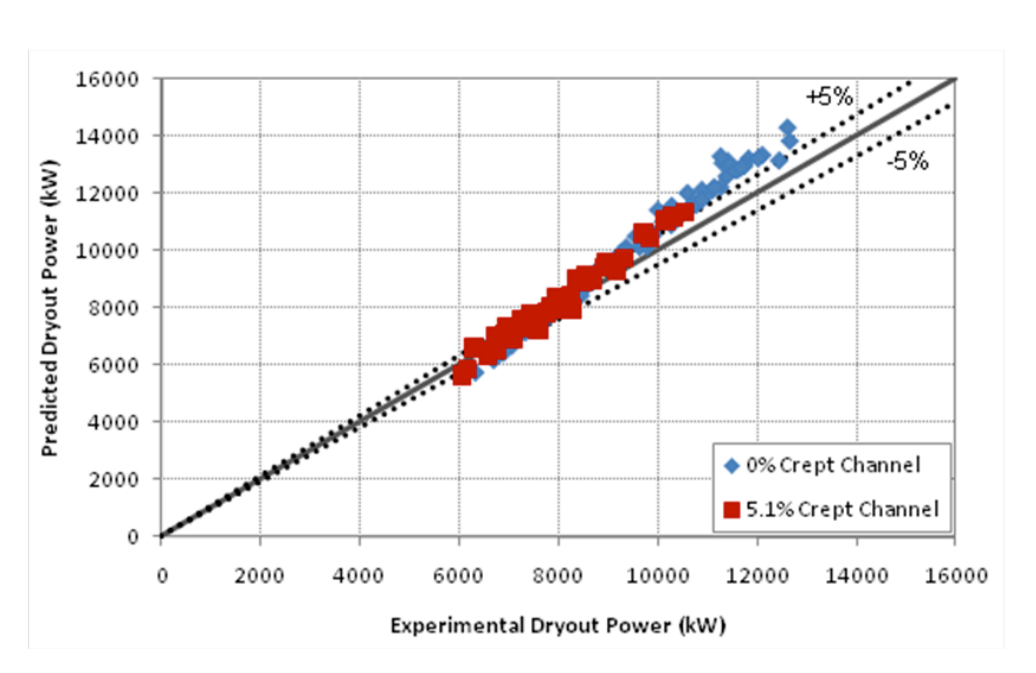


Figure 7: Comparison of Measured and Predicted Dryout Powers for 0% and 5.1% Crept Channels

The CHF prediction capability of ASSERT-PV was also assessed against the experimental CHF with respect to the cross sectional average local flow conditions (i.e., quality, pressure, and mass flux). As the axial power profile is non-uniform, the BLA approach was used for the calculation of CHF, instead of the local method. The BLA CHF is defined as:

$$CHF_{BLA} = \frac{1}{z_{DO} - z_{OSV}} \int_{z_{OSV}}^{z_{DO}} q_{local} dz \tag{4}$$

where z_{DO} and z_{OSV} are the axial locations of the dryout and onset of significant void (OSV) points, respectively, in metres, and q_{local} is the local heat flux in kW m⁻². The location of OSV is determined by comparing the local thermodynamic quality against the predicted value at OSV. The dryout quality at the location of dryout is calculated through a heat balance and is expressed as:

$$x_{DO} = \frac{1}{H_{fg}} \left(\frac{Power_{local}}{W} + H_{in} - H_{f} \right)$$
(5)

where $Power_{local}$ is the local power at the dryout location calculated via integration of the axial power between inlet and the dryout locations, in kW, and H_{in} , H_f and H_{fg} are the inlet flow enthalpy, local saturated liquid enthalpy, and latent heat of vaporization, respectively, in kJ kg⁻¹.

Figure 8 compares experimental and predicted BLA CHF values. ASSERT-PV tends to slightly overpredict the CHF values in the uncrept channel, and to underpredict in the 5.1% crept channel. The overall average error is -1.4% and the associated uncertainty is 8.6% for all data, -8.7% and 7.3% for the 5.1% crept channel, and 2.7% and 6.2% for the uncrept channel, respectively.

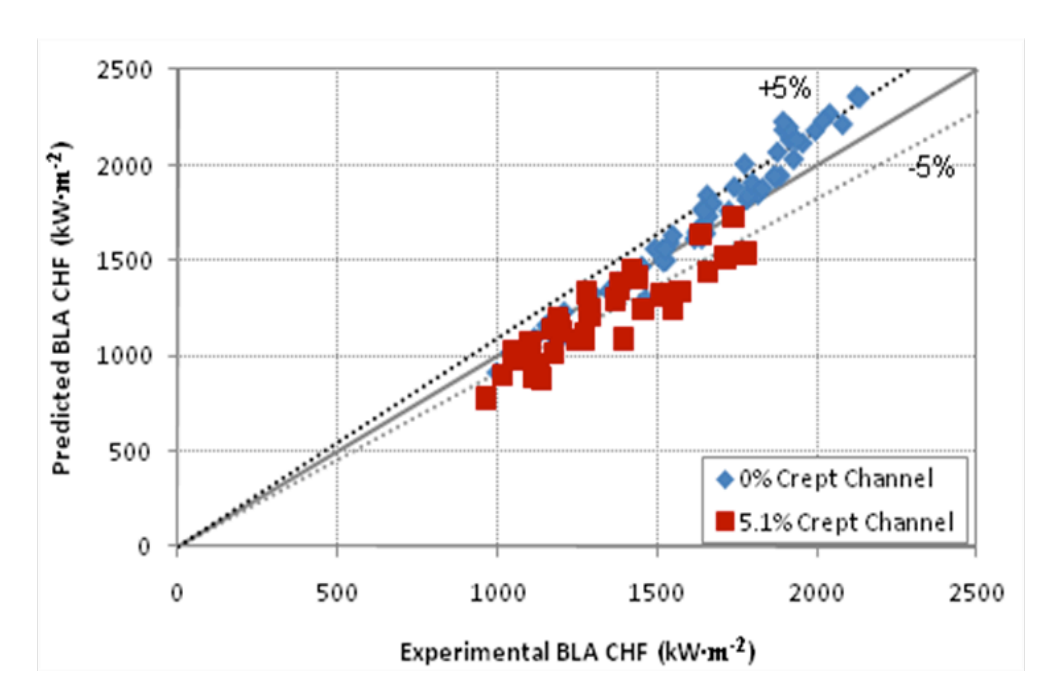


Figure 8: Comparison of Experimental and Predicted BLA CHF for 0% & 5.1% Crept Channels

4.2 Generation of CANFLEX Bundle Data for Subcooled Boiling Region Using ASSERT-PV The ASSERT-PV code was used to predict dryout powers in slightly to moderately subcooled boiling regions. Simulations were only carried out for 5.1% crept channel, because the dryout takes place earlier in the crept channel (at lower qualities) in comparison to the uncrept channel at similar flow conditions. Critical heat fluxes and cross-sectional average local flow conditions at the dryout location were then calculated from the dryout power and the axial dryout location. The simulation covered pressures of 9, 10, 11, and 12 MPa, inlet temperatures of 100, 150, 200, and 250°C, and mass-flow rates of 17, 19, 21, and 23 kg s⁻¹.

Figure 9 shows the variation of dryout power with the inlet fluid temperature, outlet pressure and the mass-flow rate. Dryout power decreases with decreasing mass-flow rate. The effect of mass flow rate is higher at low inlet temperatures than at higher inlet temperatures. The pressure effect on dryout power is almost negligible. ASSERT-PV was also used to predict the dryout power in a bundle string with 1.7 mm bearing pad height at flow conditions including outlet pressures of 9 and 11 MPa, inlet temperatures of 100, 200 and 250°C, and mass flow rate of 21 kg s⁻¹. The average relative difference in the predicted dryout powers between CANFLEX bundles with 1.7 mm and 1.8 mm bearing pads is 0.58%, with a standard deviation of 0.07. Therefore, the difference is negligible.

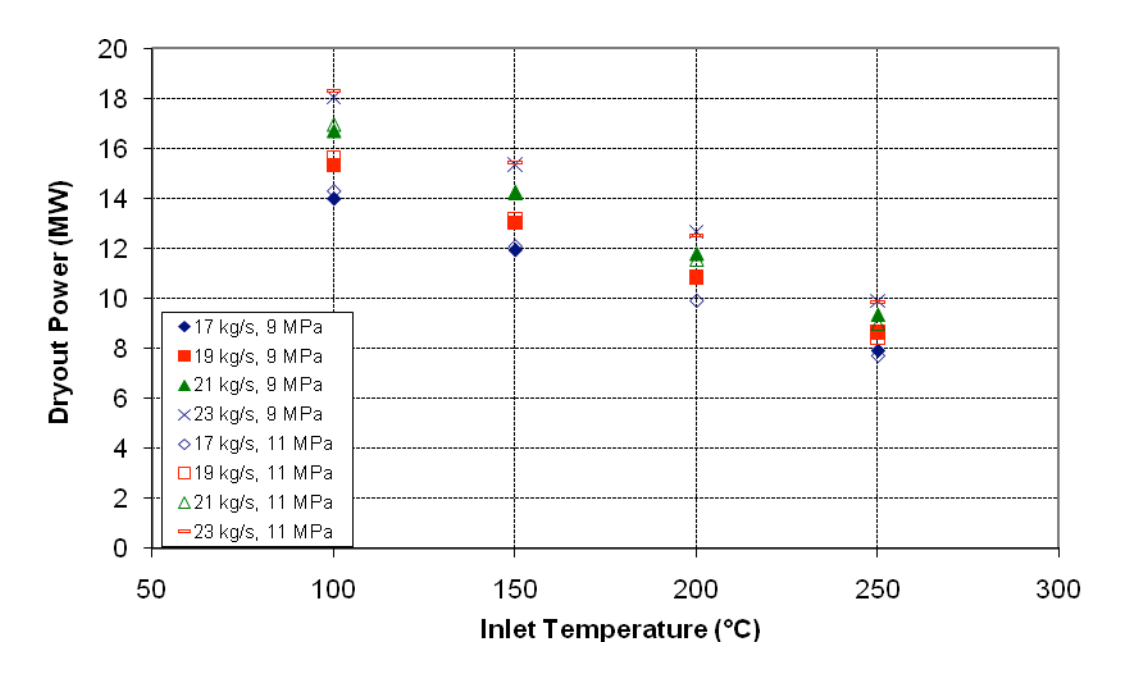


Figure 9: Variation of Dryout Power with Inlet Temperature, Outlet Pressure and Mass-Flow Rate

4.3 Verification of the Trend for ASSERT Generated Data

CHF values predicted using the ASSERT-PV code have been examined for bias and other effects, which may cause deviation from the available experimental data. The ASSERT-PV simulations were carried out for the 5.1% crept channel. Predicted CHF values were converted to uncrept channel equivalent values for establishing the reference CHF trend. The conversion from crept channel BLA CHF to uncrept channel equivalent values was based on the creep factor developed with the SL experimental data, which is expressed as:

$$K_{creep} = \frac{CHF_{crept}}{CHF_{uncrept}} = \exp\left[-2.19\left(1 - \frac{1 - \varepsilon}{1 - \varepsilon_{uncrept}}\right)\right]$$
 (6)

where the bundle eccentricity, ε , is defined as:

$$\varepsilon = \frac{D_{PT} - D_{bundle}}{D_{PT} - D_{inner}} \tag{7}$$

where D_{PT} is the pressure-tube inner diameter in metres, D_{bundle} is the overall bundle diameter in metres, and D_{inner} is the equivalent inner-tube diameter of an annulus in metres. The equivalent inner-tube diameter in annuli representing the bundle, D_{inner} , is calculated with:

$$D_{inner} = d_{cr} + \frac{7D_{ir}d_{ir}^2 + 14D_{mr}d_{mr}^2 + 21D_{or}d_{or}^2}{7d_{ir}^2 + 14d_{mr}^2 + 21d_{or}^2}$$
(8)

where D_{ir} , D_{mr} , and D_{or} are the pitch-circle diameters of the inner-, middle- and outer-rings, respectively, in metres, and d_{cr} , d_{ir} , d_{mr} , and d_{or} are the element diameters of the center rod, inner-, middle- and outer-ring, respectively, in metres. The overall bundle diameter, D_{bundle} , is calculated using:

$$D_{bundle} = D_{or} + d_{or} + 2t_{bp} \tag{9}$$

where t_{bp} is the bearing pad height in metres. The bundle eccentricity in the uncrept channel, $\varepsilon_{uncrept}$, is calculated with Equation 7 based on the uncrept pressure-tube diameter.

The uncrept channel equivalent BLA CHF values were then compared to the SL uncrept channel BLA CHF values for bias. The comparison was restricted to the qualities above 0%, because no data below 0% quality exists in the SL uncrept channel tests. The predicted BLA CHF values were systematically lower than the SL BLA CHF values (both with 1.7 mm and 1.8 mm bearing pads) at similar dryout qualities. The following correction has been introduced to eliminate this systematic bias,

$$K_{bias} = \frac{CHF_{bias}}{CHF_{unbias}} \tag{10}$$

where CHF_{bias} and CHF_{unbias} are the BLA CHF values with and without systematic bias. To facilitate the comparison at the same local critical flow conditions, a correlation has been derived, with a form expressed as:

$$CHF_{unbias} = 4.306P^{-0.675}G^{0.609} - 9.146P^{-1.055}G^{1.140}x_{Do}$$
 (11)

where P is the local pressure in MPa, G is the local mass flux in Mg m⁻² s⁻¹, and x_{DO} is the dryout quality.

The coefficients were optimized using the SL uncrept channel CANFLEX bundle data obtained with 1.7 mm bearing pad height. The average error and standard deviation for the optimization of BLA CHF values were 0.82% and 4.87% for 100 data points. The average correction factor was calculated to be 0.87 and applied to all predicted uncrept channel equivalent BLA CHF values. Figure 10 shows that the BLA CHF is improved after applying the correction factor.

5. BLA CHF CORRELATION

The CHF correlation for the subcooled boiling region was derived using BLA CHF and local conditions calculated based on dryout powers established using ASSERT-PV (as described in the

previous section). This correlation has been coupled with the correlation developed for the bulk boiling region to cover the regions from subcooled to bulk boiling.

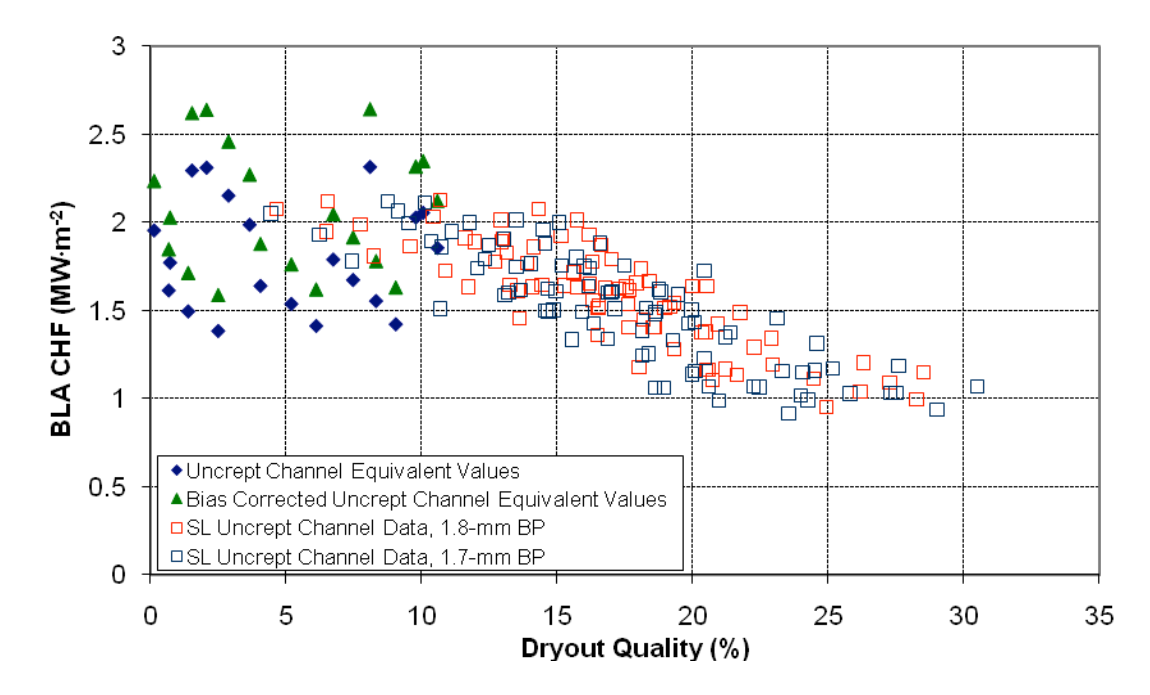


Figure 10: Comparison of SL Uncrept Channel BLA CHF with Bias Uncorrected/Corrected (Uncrept Channel Equivalent) Predicted Values

5.1 Update of the CANFLEX CHF Correlation

The updated BLA CHF correlation includes two parts, and selects the maximum of these two CHF calculations. The first part (CHF_{subcooled}) was derived using the ASSERT predictions at low qualities and in the subcooled boiling region. The second part is the existing (reference) correlation (CHF_{ref}) which was derived using CANFLEX Mk-V data for a 1.7 mm bearing pad.

$$CHF_{BLA} = \max(CHF_{ref}, CHF_{subcooled})$$
 (12)

5.1.1 CHF Correlation For Subcooled Boiling Region (CHF_{subcooled})

The BLA CHF correlation derived for the subcooled region is expressed as:

$$CHF_{subcooled} = aP^bG^c + dP^eG^f x_{Do}$$
 (13)

where P is the local pressure in MPa, G is the local mass flux in Mg m⁻² s⁻¹ and x_{DO} is the dryout quality. The coefficients in Equation 13 were optimized using ASSERT-PV predictions after applying the creep factor (Equation 3) to convert crept channel data (ASSERT-PV predictions) into uncrept channel equivalent values and the bias correction (Equation 10) to correct with respect to the SL CANFLEX uncrept channel data.

5.1.2 Reference CHF (CHF_{ref}) Correlation

The non-dimensional CHF correlation is expressed as:

$$Bo = \frac{CHF_{ref}}{GH_{fg}} = \frac{1}{10000} \left(b_1 \left(\frac{\rho_f}{\rho_g} \right)^{b_2} We_{\text{mod}}{}^{b_3} - b_4 \left(\frac{\rho_f}{\rho_g} \right)^{b_5} We_{\text{mod}}{}^{b_6} x_{DO} \right)$$
(14)

where G is the local mass flux in kg m⁻² s⁻¹, H_{fg} is the latent heat of vaporization in J kg⁻¹, ρ_f and ρ_g are the saturated-liquid and saturated-vapour densities respectively in kg m⁻³, and x_{DO} is the thermodynamic quality at the dryout location. The BLA CHF is defined in Equation 1. The modified Weber number, We_{mod} , in Equation 14 is defined as:

$$We_{\text{mod}} = \frac{GD_{hy}^{0.5}}{\rho_f^{0.5}\sigma^{0.5}}$$
 (15)

where D_{hy} is the hydraulic-equivalent diameter in metres, and σ is the surface tension in N m⁻¹. The coefficients in Equation 15 are expressed as:

$$b_{1} = a_{1} \left(\frac{1 - E}{1 - E_{uncrept}} \right)^{a_{7}}; \qquad b_{2} = a_{2} + a_{8} \left(1 - \frac{1 - E}{1 - E_{uncrept}} \right);$$

$$b_{3} = a_{3} + a_{9} \left(1 - \frac{1 - E}{1 - E_{uncrept}} \right); \qquad b_{4} = a_{4} + a_{10} \left(1 - \frac{1 - E}{1 - E_{uncrept}} \right);$$

$$b_{5} = a_{5} + a_{11} \left(1 - \frac{1 - E}{1 - E_{uncrept}} \right); \qquad b_{6} = a_{6} + a_{12} \left(1 - \frac{1 - E}{1 - E_{uncrept}} \right).$$

$$(16)$$

where the coefficients $(a_1 - a_{12})$ were optimized using the SL CANFLEX data.

5.2 Predictions of CHF Correlation

The CHF correlation in Equation 12 has been assessed against the SL CANFLEX data.

Table 1 summarizes the dryout power prediction accuracy for the CANFLEX bundle with 1.7 mm and 1.8 mm bearing pads. Dryout powers are underpredicted in the uncrept channel for 1.7 mm and 1.8 mm bearing pad heights, slightly overpredicted in the crept channel(s) for the 1.7 mm bearing pad height, and slightly underpredicted for the 1.8 mm bearing pad height.

Overall, the data are underpredicted, with the average prediction error being less than 1% for the bundle with 1.7 mm bearing pad height, and less than 3.5% for the bundle with 1.8 mm bearing pad height. In both cases, the standard deviation is less than 3%. Figure 12 compares SL dryout power data with the predictions of the correlation for the uncrept and crept channels. In general, the predictions lie within the error bands of $\pm 5\%$.

Table 1: Prediction Accuracy of the Correlation for Dryout Power

	1.7 mm Bearing Pad Height				1.8 mm Bearing Pad Height			
Channel maximum creep	0%	3.3%	5.1%	all	0%	5.1%	all	
Number of data	75	50	46	171	69	38	107	
Average error (%)	-2.28	1.19	0.97	-0.39	-4.81	-0.84	-3.35	

Standard Deviation (%)	1.30	1.96	2.25	2.45	1.46	2.30	2.64
------------------------	------	------	------	------	------	------	------

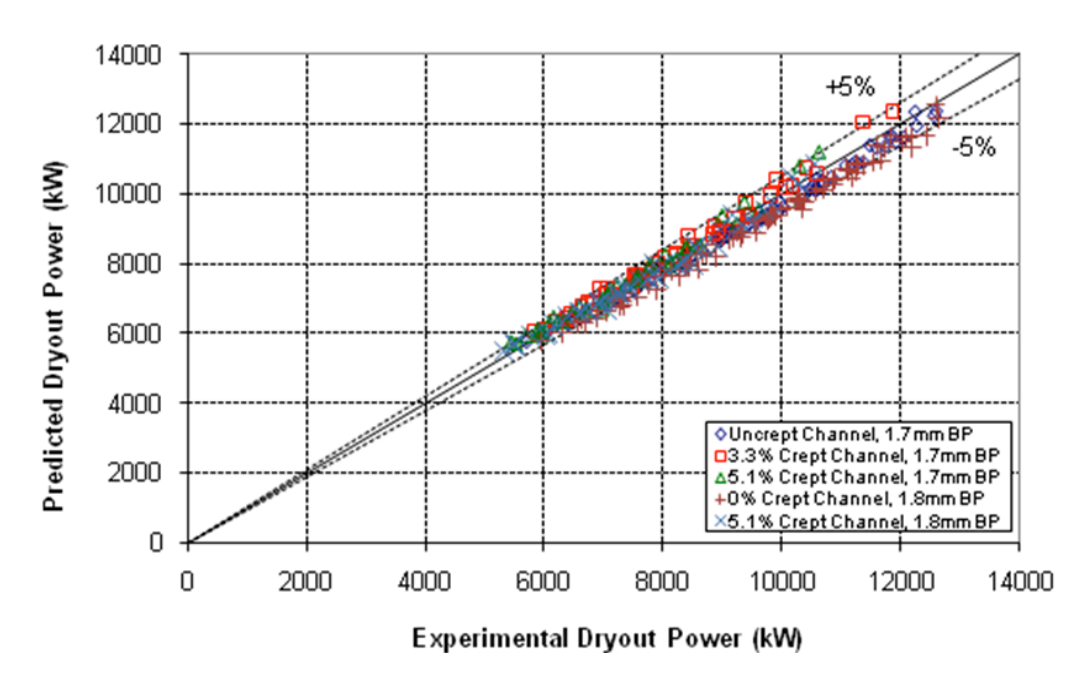


Figure 12: Comparison of SL Dryout Power Data with the Predictions of the Correlation for the CANFLEX bundle with 1.7 mm and 1.8 mm Bearing Pad Heights

6. CONCLUSION

The existing CHF correlation has been updated to broaden its application range. The ASSERT-PV subchannel code has been used to generate data in the low quality and subcooled boiling regions. The trend of the data was verified against the SL uncrept channel data for any bias. Using the generated data, a correlation has been derived and combined with the existing CANFLEX CHF correlation. The updated correlation (the combination of these two correlations) has then been assessed against SL uncrept and crept channel data for the prediction of dryout powers.

Overall, the data are underpredicted with the average prediction error being less than -1% for the bundle with 1.7 mm bearing pad height, and less than -3.5% for the bundle with 1.8 mm bearing pad height. In both cases, the standard deviation is less than 3%.

7. REFERENCES

- [1] L.K.H. Leung, "Effect of CANDU Bundle-Geometry Variation on Dryout Power", Journal of Engineering for Gas Turbines and Power, Vol. 131, No. 2, pp. 35-45, 2009.
- [2] M.B. Carver, J.C. Kiteley, A. Tahir, A.O. Banas, and D.S. Rowe, "Simulation of Flow and Phase Distribution in Vertical and Horizontal Bundles using the ASSERT Subchannel Code", *Nuclear Engineering and Design*, **122**, pp. 413-424, 1990.
- [3] Y.F. Rao and N. Hammouda, "Recent Development in ASSERT-PV Code for Subchannel Thermalhydraulics", *Proceeding of the 8th CNS Int. Conf. on CANDU Fuel*, Sep 21-24, Honey Harbor, Ontario, 2003.
- [4] Y. Rao and L.K.H. Leung, "Thermalhydraulics Performance Optimization of CANDU Fuel Using ASSERT Subchannel Code", *Proceeding of the 2007 International Congress on Advances in Nuclear Power Plants*, May 13-18, Nice Acropolis, France, 2007.
- [5] G.R. Dimmick, W.W.R. Inch, J.S. Jun, H.C. Suk, G. Haddaller, R. Fortman, and R. Hayes, "Full-Scale Water CHF Testing of the CANFLEX Bundle," *Proceedings of the 6th Int. Conf. on CANDU Fuel*, Niagara Falls, Ontario, 1999.

- [7] L.N. Carlucci, N. Hammouda and D.S. Rowe, "Two-Phase Turbulent Mixing and Buoyancy Drift in Rod Bundles," *Nuclear Engineering and Design*, **227**, pp. 65-84, 2004.
- [8] D.C. Groeneveld, L.K.H. Leung, P.L. Kirillov, V.P. Bobkov, I.P. Smogalev, V.N. Vinogradov, X.C. Huang and E. Royer, "The 1995 Look-Up Table for Critical Heat Flux in Tubes", *Nuclear Engineering and Design*, **163**, pp. 1-23, 1996.